Electronic supporting information (ESI)

Polymeric copper(II) and dimeric oxovanadium(V) complexes of amide-imine conjugate: bilirubin recognition and green catalysis

Jayanta Das[a], Sabyasachi Ta[a], Sudipta Das[b], Noor Salam[a,c], Subhasis Ghosh[a], and Debasis Das[a]*

[a]*Department of Chemistry, The University of Burdwan, Burdwan, 713104, W.B., India*
[b]*Raina Swami Bholananda Vidyayatan, Burdwan,713421, W.B., India*
[c]*Department of Chemistry, Surendranath College, 24/2 MG Road, Kolkata, 700009, WB, India*
E-mail: ddas100in@yahoo.com (D. Das)

Materials and methods

All experiments were carried out in aerobic conditions. High-purity PBS buffer, hydrazine hydrate, 4-methyl-1-benzoic acid, thionyl chloride,4-(*N,N*-Diethyl amino)salicylaldehyde and Bilirubin are purchased from Sigma Aldrich (India). $Cu(OAc)_2$, $VOSO_4$, NaOH were purchased from Merck (India) were of reagent grade. Solvents used are of spectroscopic grade. Other chemicals are of AR grade and have been used without further purification except when specified. Mili-Q Milipore 18.2 MΩ cm^{-1} water has been used throughout all the experiments.

Elemental analyses (C, H, and N) were performed using a PerkinElmer 2400 series II CHN analyzer. FTIR spectra are recorded on a Shimadzu FTIR (model IR Prestige 21 CE) spectrophotometer. The electronic absorption spectra are collected with A Shimadzu Multi Spec 2450 spectrophotometer.Path length of the cells used for absorption studies is 1 cm. Fluorescence spectra was taken on Hitachi F-7000 spectrofluorometer. A Bruker ADVANCE III HD (400 MHz) spectrometer was employed to record ^1H NMR and ^{13}C NMR spectra using DMSO-d_6 and $CDCl_3$ as solvent, the chemical shift was represented in ppm with residual solvent peak was used as an internal reference. Multiplicity was indicated as follows: s (singlet), d (doublet), t (triplet), q (quartet), m (multiplet). Coupling constants (*J*, s) were reported in Hertz (*Hz*). A QTOF 60 Micro YA 263 and mass spectrometerwas employed to measure the mass spectrum in the ES positive mode. Solutions of compounds were injected at a flow rate of 5 μL/min. Systronics digital pH meter (model 335) is used for measurement of solution pH. Dilute HCl or NaOH (50 μM) are used for pH adjustment.GC analysis were performed using Varian 3400 gas chromatograph equipped with a 30 m CP-SIL8CB capillary column and a Flame Ionization Detector.

The X-ray data were collected on a Bruker X8 APEXII CCD diffractometer at 100(2) K, using graphite-monochromated Mo-Ka radiation (l ¼ 0.71073 °A). Some significantcrystal parameters and refinement data are furnished in Table S1 (ESI). Data were processed and corrected for Lorentz and polarization effects. Standard direct methods[1] are used for solving the structures and refined by full matrix least squares on F^2.[2] All non-hydrogen atoms were anisotropically refined. Hydrogen atoms were included in the structure factor calculation in geometrically idealized positions, with thermal parameters depending on the parent atom, using a riding model.Images were generated by ORTEP and Mercury software.

General method of UV-Vis and fluorescence titration

Path length of the cells used for absorption and emission studies is 1 cm. For UV-Vis and fluorescence titrations, stock solution of **C1** is prepared (20 μM) in $CHCl_3/H_2O$ medium. Working solutions of **C1** and bilirubin are prepared from their respective stock solutions. Fluorescence measurements have been performed using 5 nm × 5 nm slit width.

Job's plot from fluorescence experiment.

A series of solutions containing **C1** and bilirubin are prepared such that the total concentration of bilirubin and **C1** remained constant (20 μM) in all the sets. The mole fraction (**x**) of bilirubin is varied from 0.05 to 0.9.

Calculation of detection limit

The detection limit (**DL**) is determined from the following equation.[3]

$$DL = \frac{3\sigma}{K}$$

σ is the standard deviation of the blank solution, **K** is the slope of the calibration curve.

For the determination of standard deviation the emission intensity of **C1** without any analyte was measured by 10 times.

References

1. M. C. Burla, R. Caliandro, M. Camalli, B. Carrozzini, G. L. Cascarano, L. De Caro, C. Giacovazzo, G. Polidori, R. Spagna, *J. Appl. Cryst.*, 2015, **48**, 306-309.

2. Sheldrick, G. M. A short history of SHELX. *Acta Crystallographica Section A: Foundations of Crystallography*, 2008, **64**, 112.-122.

3. Zhu, M.; Yuan, M.; Liu, X.; Xu, J.; Lv, J.; Huang, C.; Liu, H.; Li, Y.; Wang, S.; Zhu, D. Visible Near-Infrared Chemosensor for Mercury Ion. *Org. Lett.*, 2008, **10**, 1481-1484.

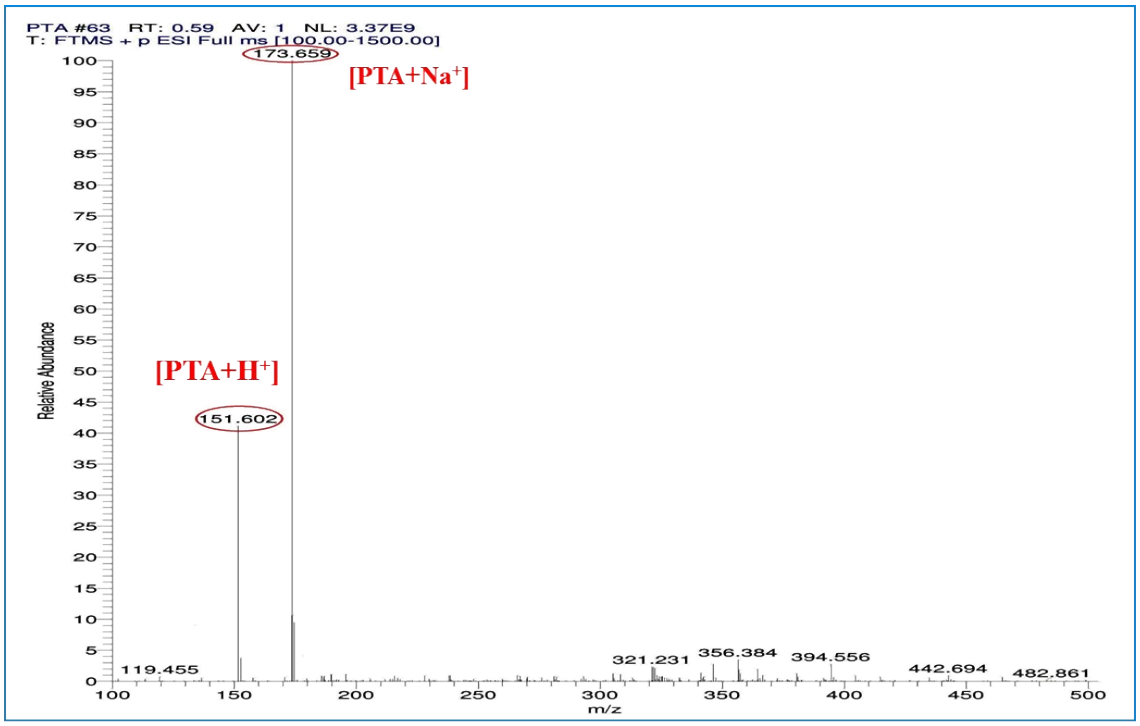

Figure S1 Mass spectrum of **PTA**

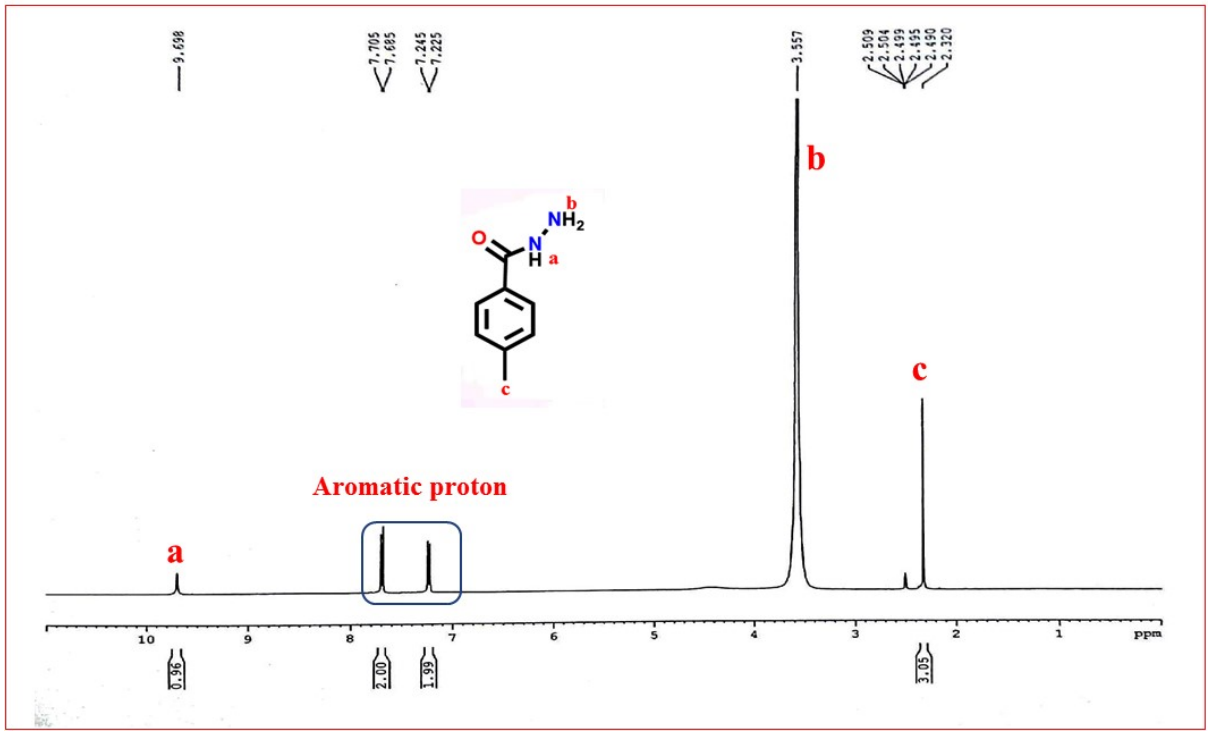

Figure S2 ^{1}H NMR spectrum of **PTA** in DMSO-d_6

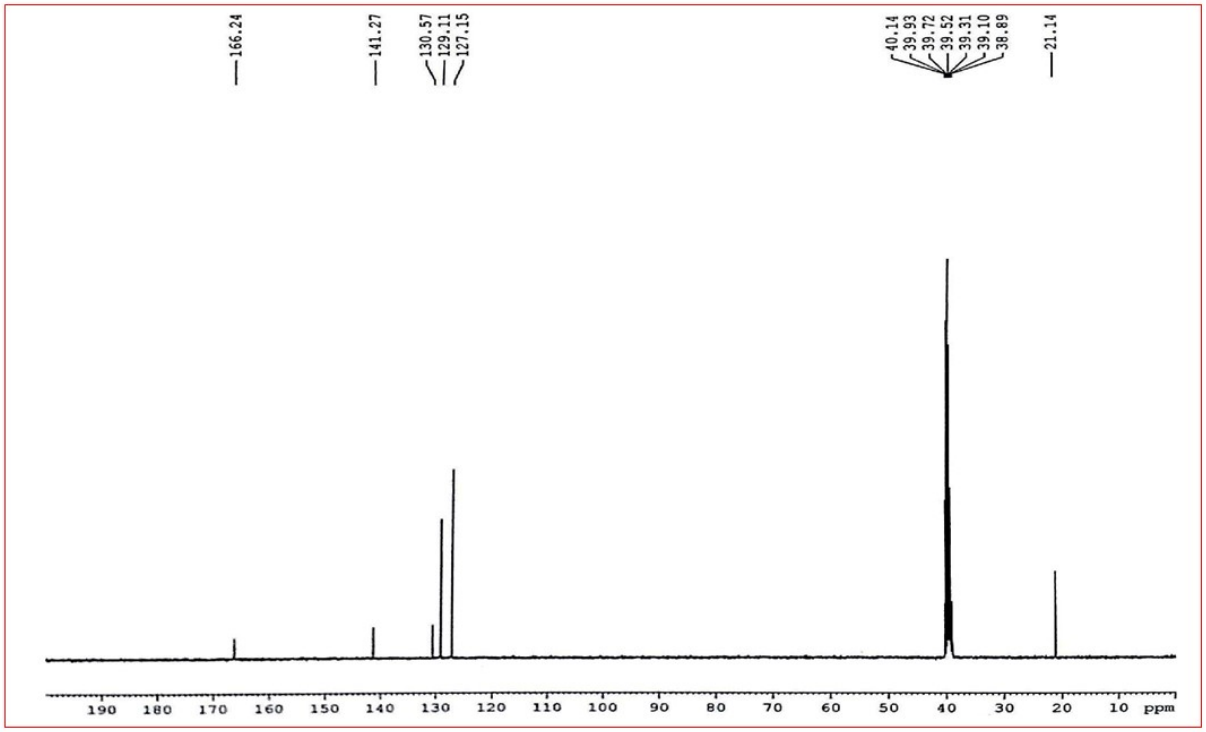

Figure S3 ^{13}C NMR spectrum of **PTA** in DMSO-d_6

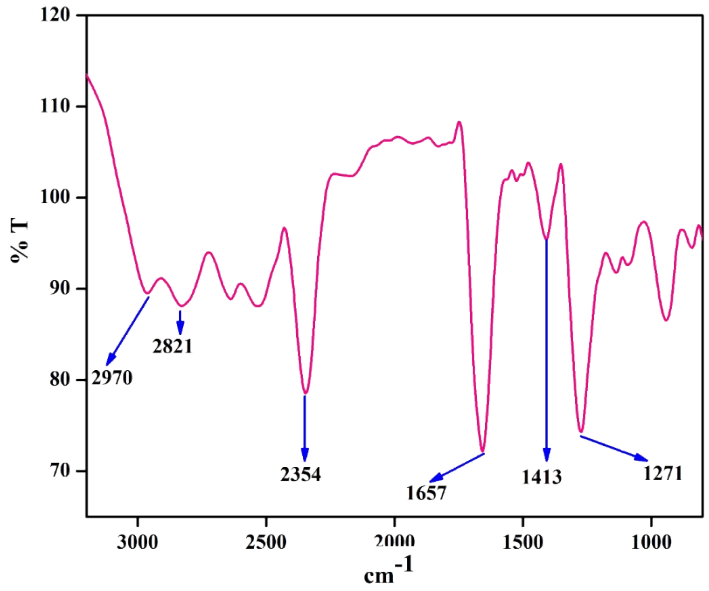

Figure S4 FTIR spectrum of **PTA**

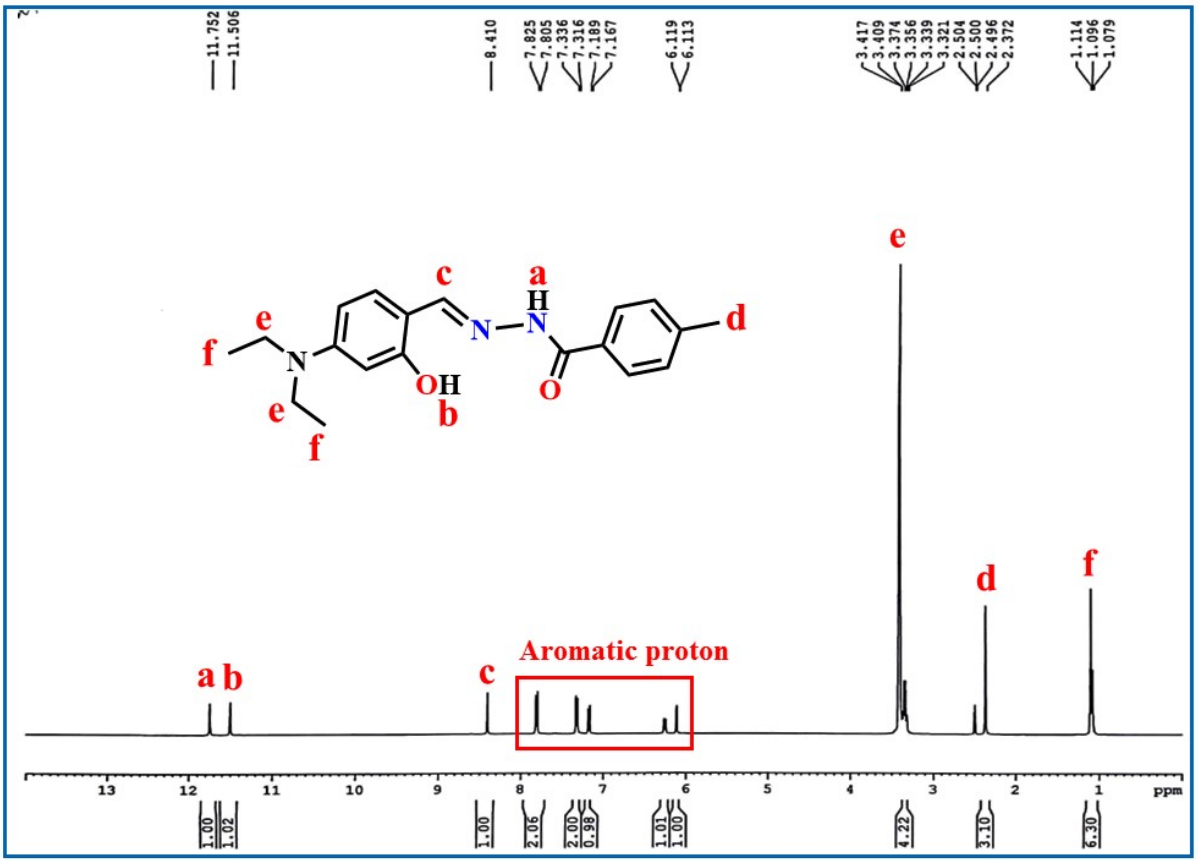

Figure S5 ^{1}H NMR spectrum of **L** in $CDCl_3$

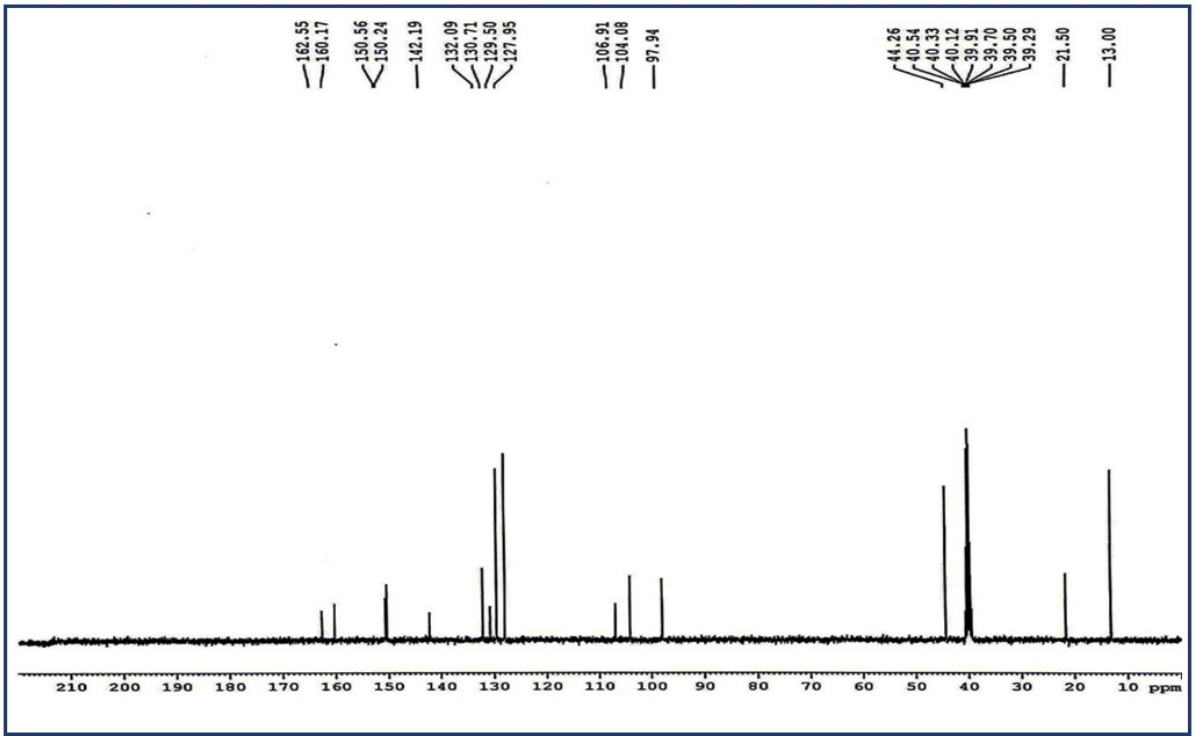

Figure S6 ^{13}C NMR spectrum of **L** in $CDCl_3$

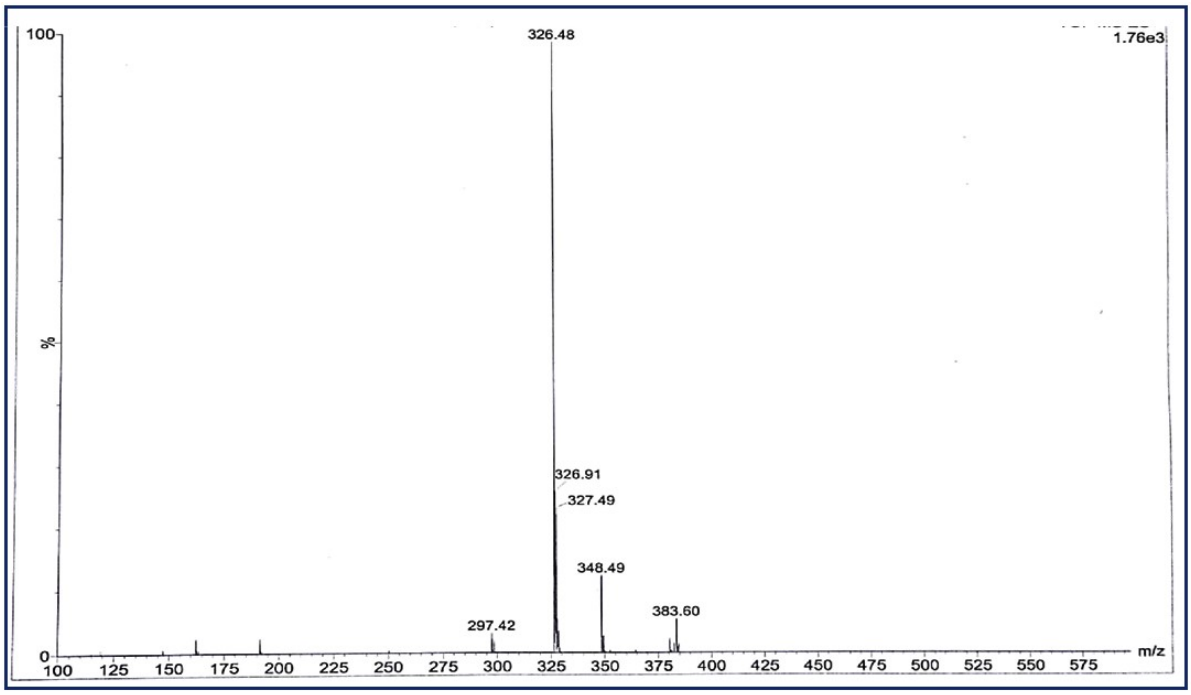

Figure S7 Mass spectrum of **L**

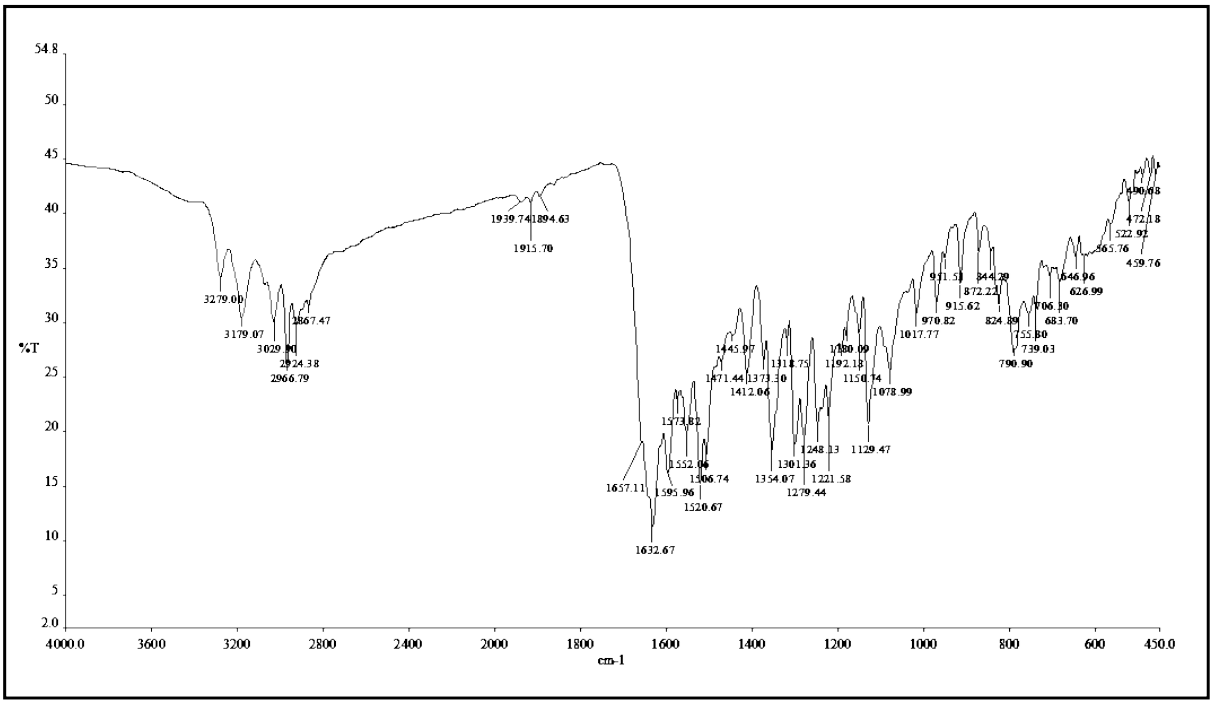

Figure S8 FTIR spectrum of **L**

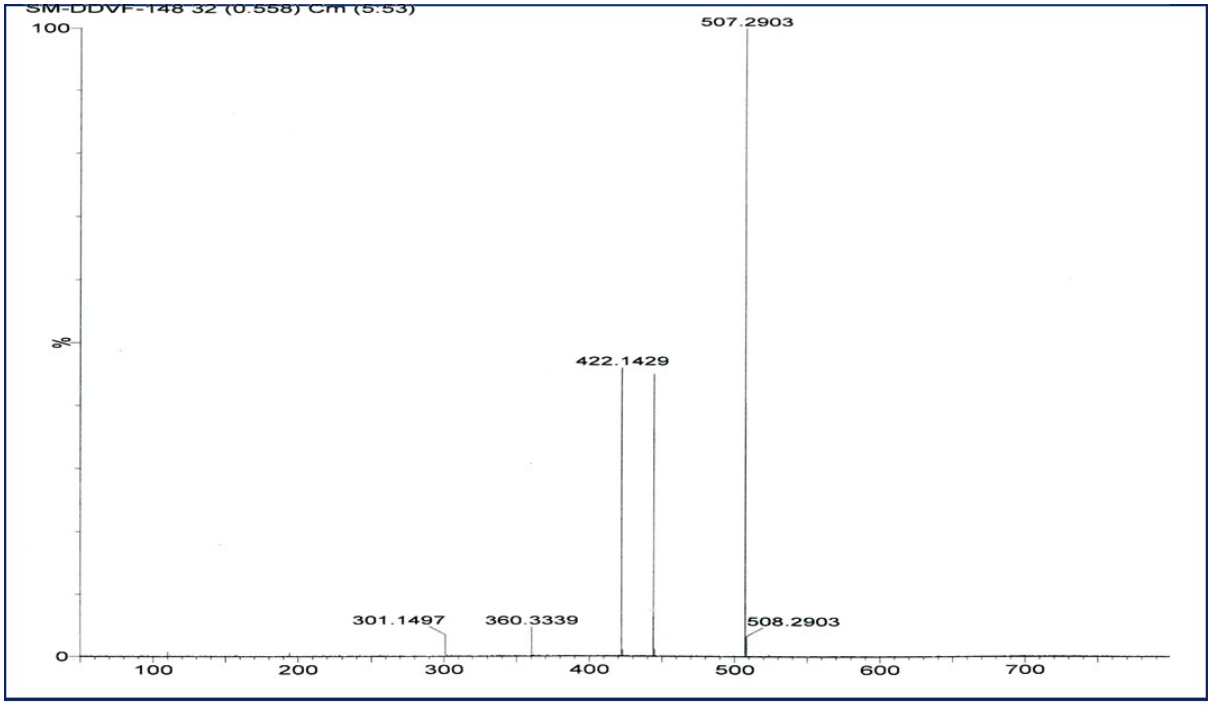

Figure S9 Mass spectrum of **V1**

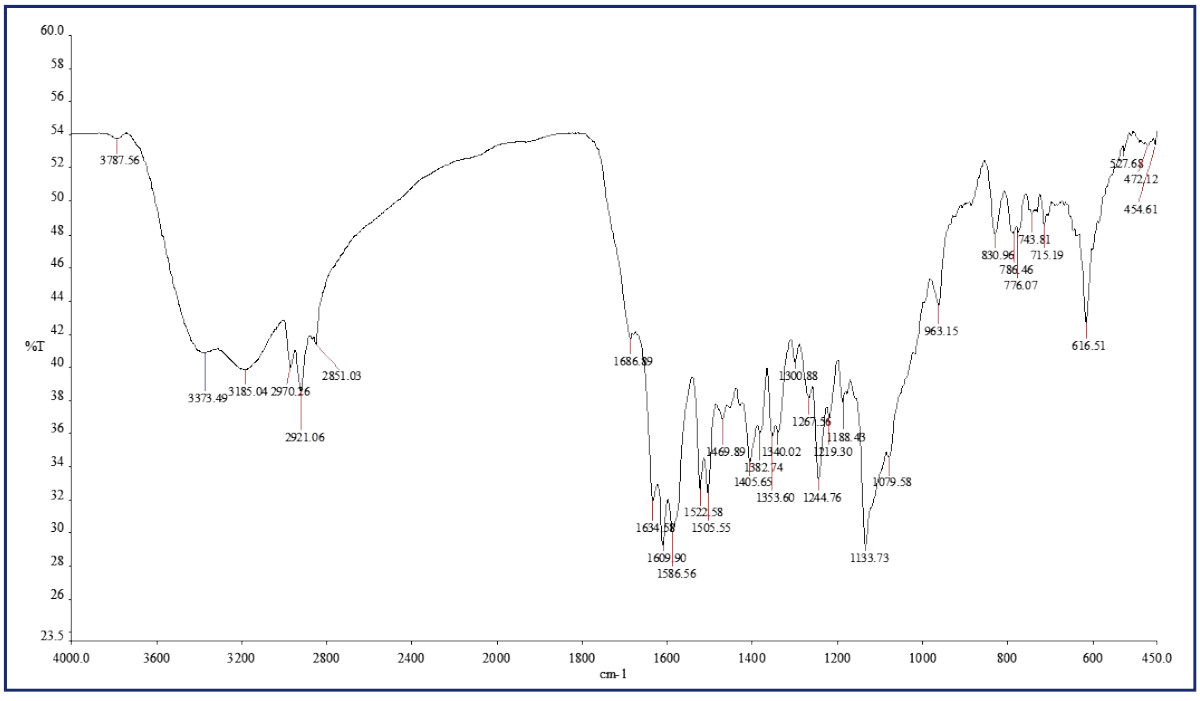

Figure S10 FTIR spectrum of **V1**

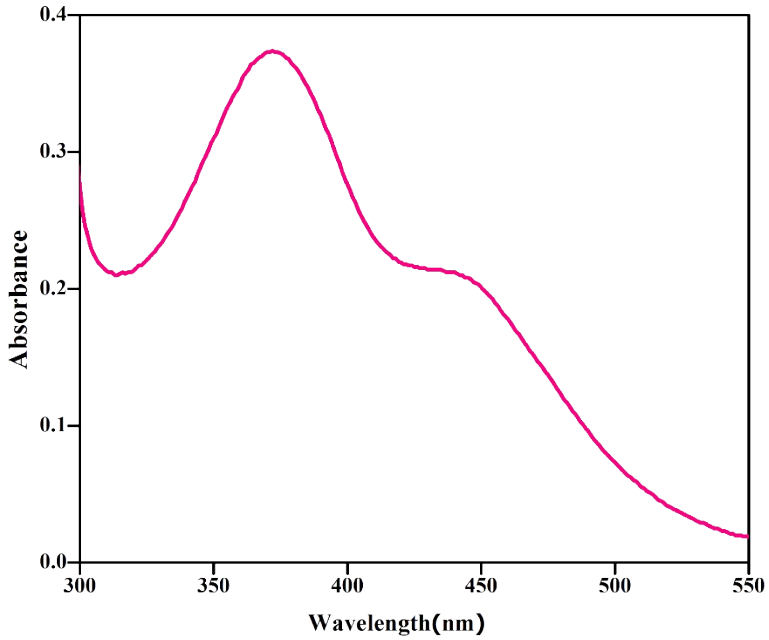

Figure S11 Absorption spectra of **V1**

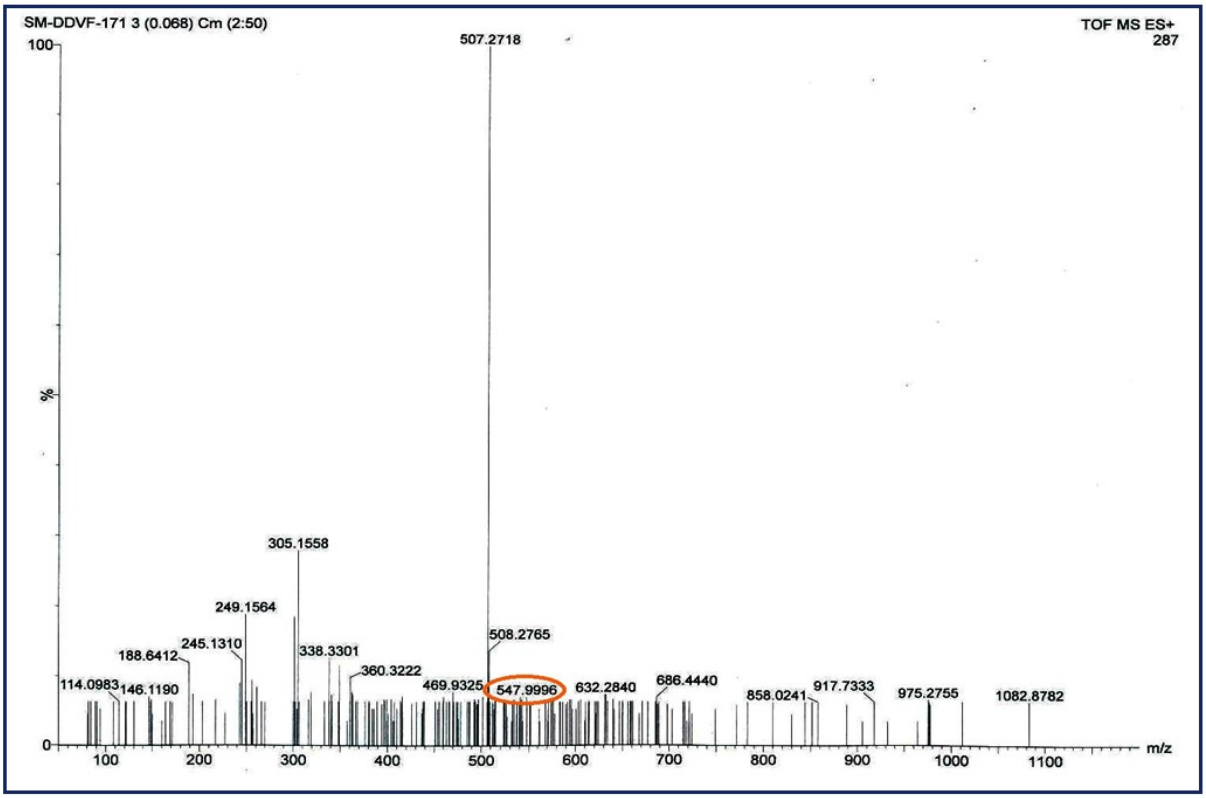

Figure S12 Mass spectrum of **C1**

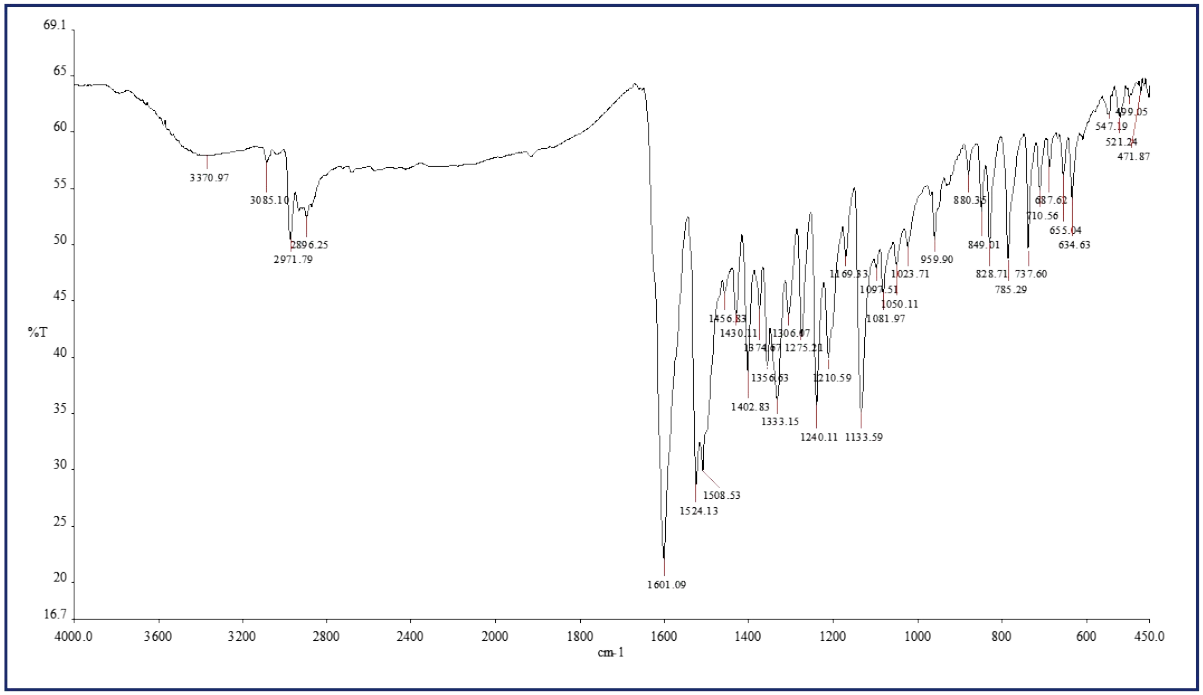

Figure S13 FTIR spectrum of **C1**

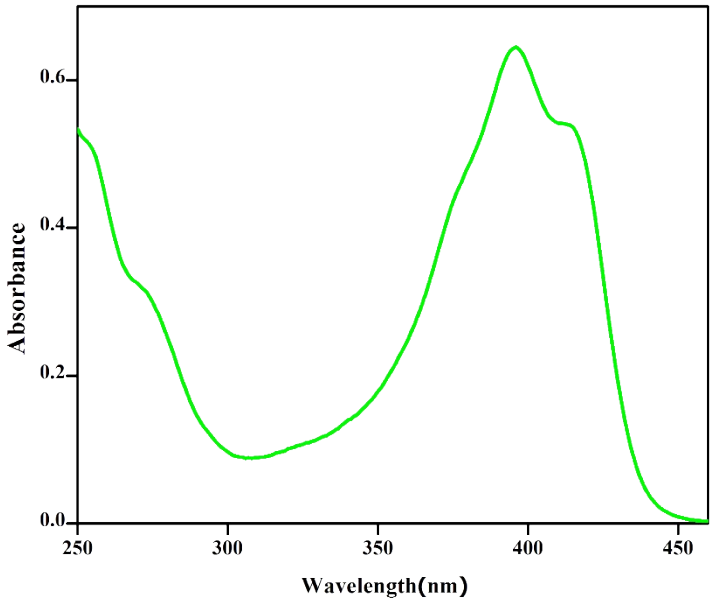

Figure S14 Absorption spectrum of **C1**

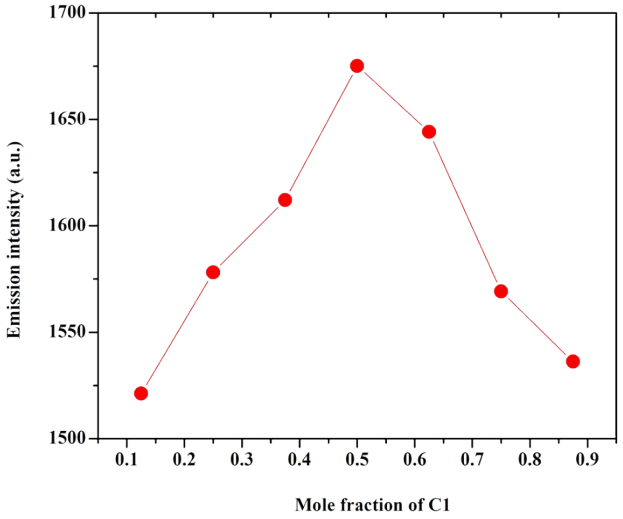

Figure S15 Job's plot for stoichiometry determination (λ_{ex}= 369 nm, λ_{em}= 444 nm)

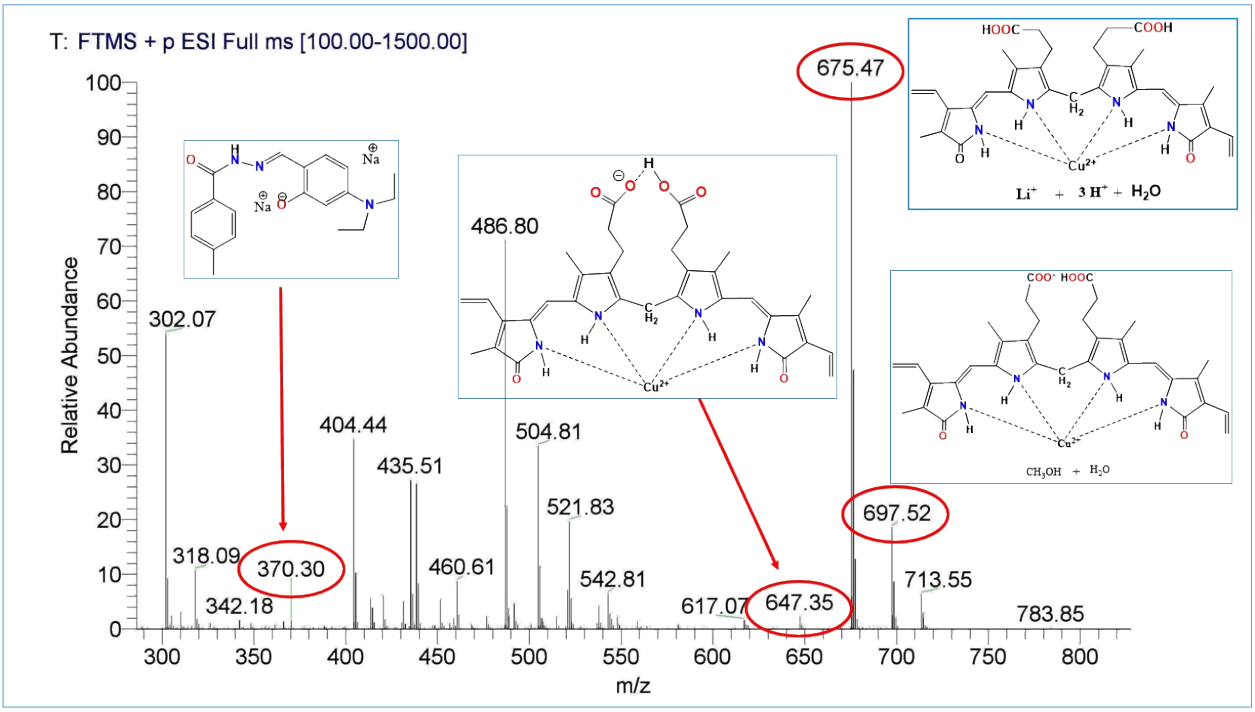

Figure S16 QTOF mass spectrum of **[C1-bilirubin]** adduct

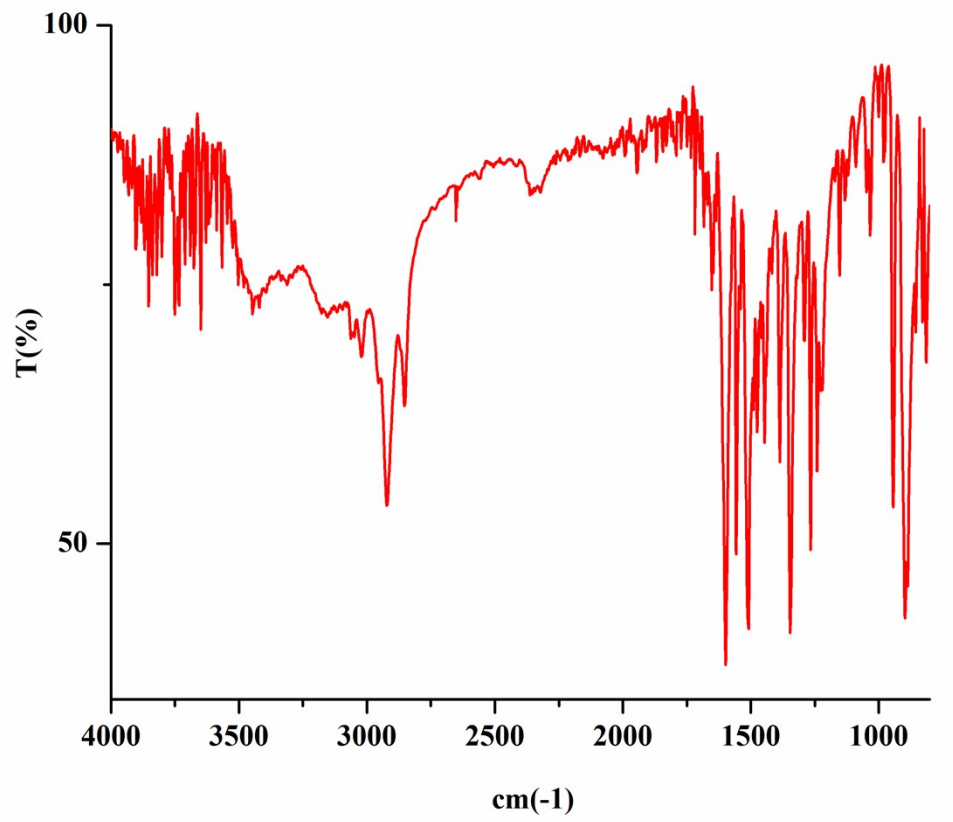

Figure S17 FTIR spectrum of **C1**-bilirubin adduct

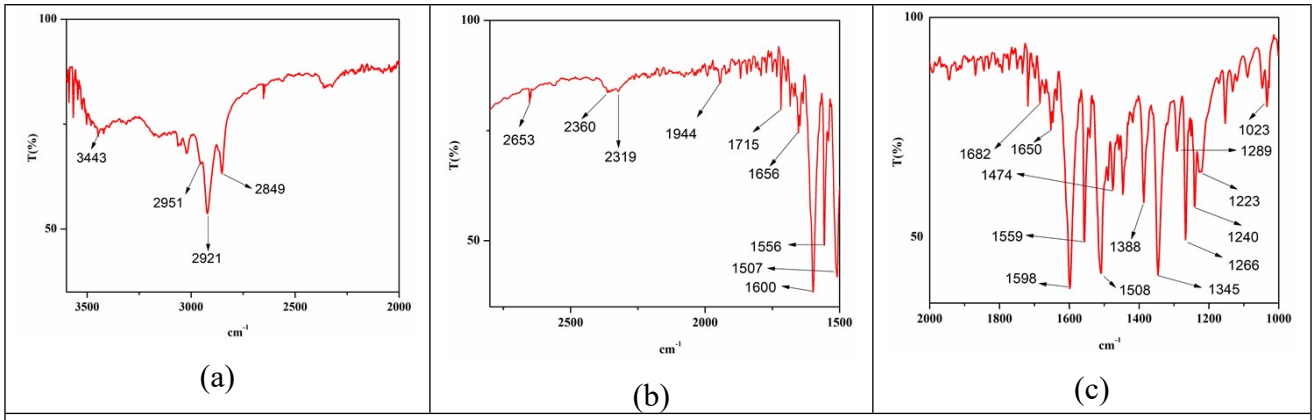

Figure S18 Enlarged view of Figure S17 (a) region: 3600-2000 cm^{-1}, (b) region: 2800-1500 cm^{-1}, (c) region: 2000-1000 cm^{-1}

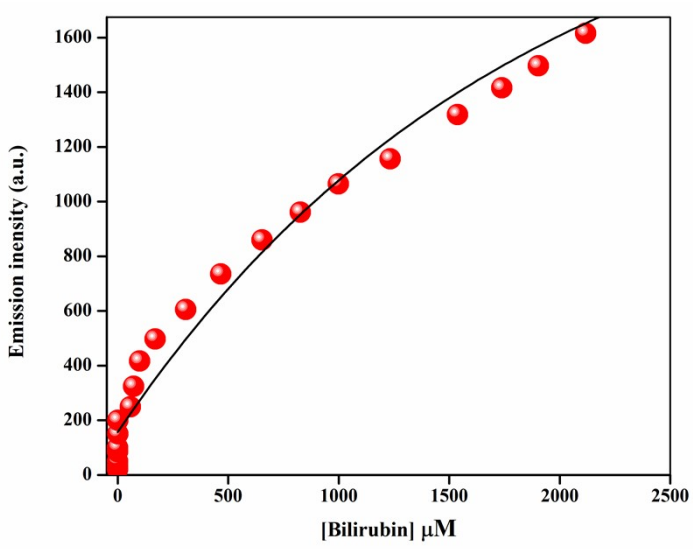

Figure S19 Plot of emission intensities of **C1** (20 µM, λ_{ex}= 369 nm, λ_{em}= 444 nm) as a function of added bilirubin (1.0-2500 µM).

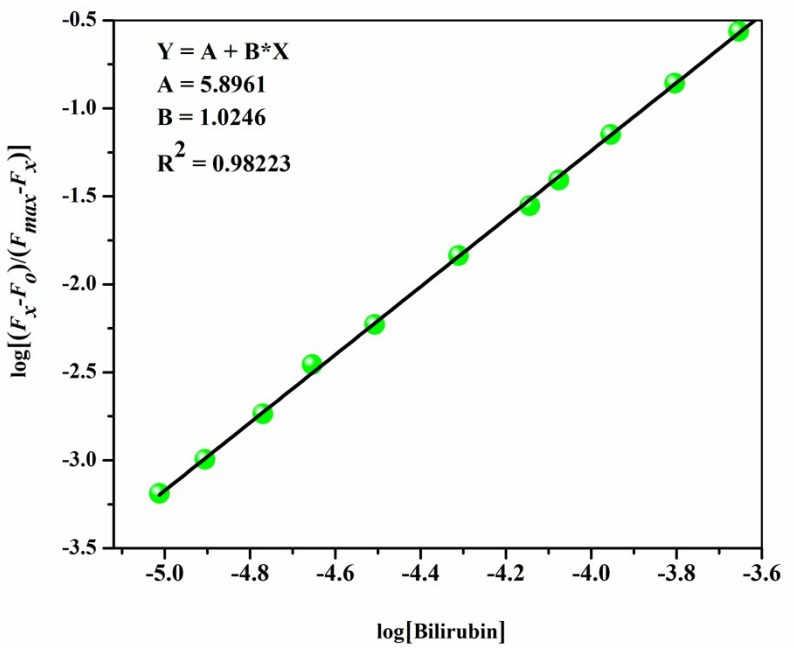

Figure S20 Hill's plot for determination of association constant of **C1** (20 µM, λ_{ex}= 369 nm, λ_{em}= 444 nm) with bilirubin (liner portion only)

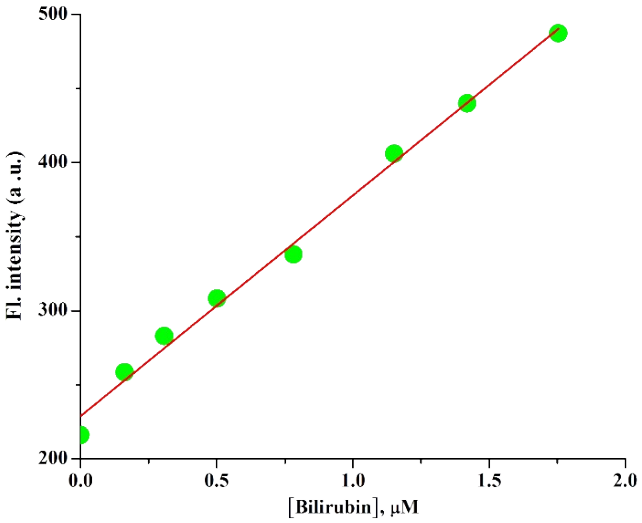

Figure S21 Determination of detection limit based on change in the emission intensity at λ_{em}= 444 nm of **C1** (20 µM) with Bilirubin(linier portion of **Figure S19)**

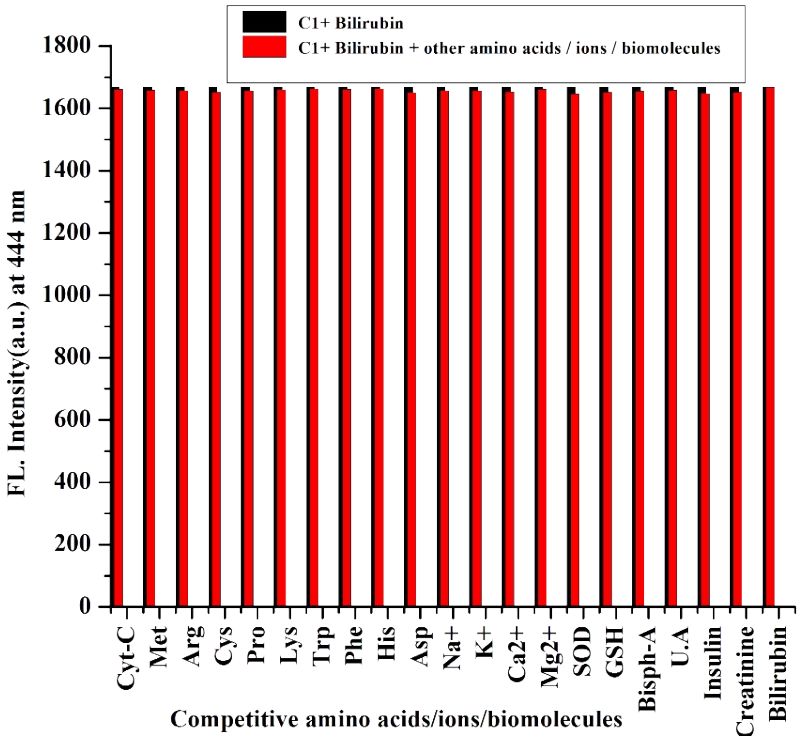

Figure S22 Plot showing interference regarding bilirubin determination using **C1** by fluorescence method (λ_{ex}= 369 nm, λ_{em}= 444 nm).

Table S1 Crystal data and structure refinement parameter for **L** and its complexes **V1** and **C1**

Crystal parameters	**L (CCDCNo.:1837665)**	**V1 (CCDC No.: 1837654)**	**C1 (CCDC No.: 1837659)**
Empirical formula	$C_{19}H_{23}N_3O_2$	$C_{40}H_{48}N_6O_8V_2$	$C_{19}H_{21}CuN_3O_2$
Formula weight	325.40 g/mol	842.72 g/mol	386.94 g/mol
Temperature	100 K	150 K	150 K
Wavelength	0.71073 Å	0.71073 Å	0.71073 Å
Crystal system	Triclinic	Triclinic	Triclinic
Space group	P -1	P -1	P -1
Unit cell dimensions	a=9.8512(6) Å; α= 94.283(5) b=11.5664(8) Å; β= 99.404(4) c = 15.7394(10) Å; γ = 102.695(4)	a= 8.146(3)Å; α= 107.404(14) b =10.585(5) Å; β= 99.533(12) c = 12.953(6) Å; γ = 106.007(13)	a = 5.8707(19) Å; α= 86.627(11) b = 11.414(4) Å; β= 77.937(10)c = 12.565(4)Å; γ = 87.756(11)
Volume	1714.6(2) $Å^3$	986.3(8)	821.6(5) $Å^3$
Z	4	1	2
Density (calculated)	1.261 g/cm^3	1.419 g/cm^3	1.564 g/cm^3
Absorption coefficient	0.083 mm^{-1}	0.534 mm^{-1}	1.347 mm^{-1}
F (000)	696.0	440.0	402.8
Theta range for data collection	2.31to28.282°	1.711to 25.654°	2.38to 27.300°
Index ranges	-13<=h<=13, -15<=k<=15, -20<=l<=20	-9<=h<=9, -12<=k<=12, -15<=l<=15	-7<=h<=7, -14<=k<=14, -16<=l<=16
Reflections collected	8498	3653	3663
Independent reflections	5290	2376	3160
Data Completeness	100 %	98.1 %	98.5%
Absorption correction	multi-scan	multi-scan	multi-scan
Refinement method	Full-matrix least-squares on F^2	Full-matrix least-squares on F^2	Full-matrix least-squares on F^2
Refinement program	SHELXL-2013 (Sheldrick, 2013)	SHELXL-2013 (Sheldrick, 2013)	SHELXL-2015 (Sheldrick, 2015)
restraints / parameters	0/448	0/257	0 / 230
Goodness-of-fit on F^2	1.042	1.046	1.041

Table S2 Selected bond lengths (Å) and bond angles (°) for **V1**

Bond lengths (Å)	Bond angles (°)	Bond angles (°)
V O4 1.597(3)	O4 V O3 100.72(14)	C4 C3 C2 120.2(4)
V O3 1.854(3)	O4 V O2 98.96(14)	C3 C4 C5 121.8(4)
V O2 1.856(3)	O3 V O2 105.25(13)	C4 C5 C6 117.6(4)
V O1 1.955(3)	O4 V O1 99.96(14)	C4 C5 C8 121.2(4)
V N2 2.090(4)	O3 V O1 90.34(13)	C6 C5 C8 121.2(5)
V O3 2.278(3)	O2 V O1 152.70(13)	C7 C6 C5 121.2(5)
O1 C1 1.333(5)	O4 V N2 97.38(15)	C6 C7 C2 120.6(4)
O2 C11 1.358(5)	O3 V N2 158.19(13)	N2 C9 C10 124.6(4)
O3 C20 1.440(5)	O2 V N2 83.69(14)	C15 C10 C11 117.1(4)
O3 V 2.278(3)	O1 V N2 74.53(13)	C15 C10 C9 121.3(4)
N1 C1 1.309(5)	O4 V O3 173.34(14)	C11 C10 C9 121.6(4)
N1 N2 1.404(5)	O3 V O3 72.72(12)	O2 C11 C12 119.1(4)
N2 C9 1.315(5)	O2 V O3 82.01(12)	O2 C11 C10 119.6(4)
N3 C13 1.363(5)	O1 V O3 81.47(11)	C12 C11 C10 121.3(4)
N3 C18 1.464(6)	N2 V O3 89.28(12)	C11 C12 C13 120.8(4)
N3 C16 1.479(5)	C1 O1 V 117.7(3)	N3 C13 C12 121.6(4)
C1 C2 1.488(6)	C11 O2 V 131.1(3)	N3 C13 C14 120.8(4)
C2 C3 1.401(6)	C20 O3 V 126.6(3)	C12 C13 C14 117.6(4)
C2 C7 1.405(6)	C20 O3 V 122.1(2)	C15 C14 C13 120.4(4)
C3 C4 1.388(6)	V O3 V 107.28(12)	C14 C15 C10122.8(5)
C4 C5 1.399(7)	C1 N1 N2 107.1(4)	N3 C16 C17 113.7(4)
C5 C6 1.404(7)	C9 N2 N1 116.1(4)	N3 C18 C19 113.3(4)
C5 C8 1.519(6)	C9 N2 V 125.8(3)	
C6 C7 1.387(6)	N1 N2 V 117.9(3)	
C9 C10 1.423(6)	C13 N3 C18 122.2(3)	
C10 C15 1.412(6)	C13 N3 C16 121.9(4)	
C10 C11 1.419(6)	C18 N3 C16 115.8(4)	
C11 C12 1.394(6)	N1 C1 O1 122.7(4)	
C12 C13 1.424(6)	N1 C1 C2 119.8(4)	
C13 C14 1.434(6)	O1 C1 C2 117.5(4)	
C14 C15 1.370(6)	C3 C2 C7 118.6(4)	

C16 C17 1.525(6) C18 C19 1.528(6)	C3 C2 C1 121.7(4) C7 C2 C1 119.7(4)	

Table S3 Selected bond lengths (Å) and bond angles (°) for **C1**

Bond lengths (Å)	**Bond angles (°)**	**Bond angles (°)**
Cu Cu 3.080(2)	O2 Cu O1 108.4(2)	C15 C10 C9 116.9(6)
Cu O1 1.982(5)	O2 Cu O1 172.71(19)	C15 C10 C11 118.0(6)
Cu O2 1.972(4)	N2 Cu O1 80.9(2)	C10 C11 O2 122.1(6)
Cu O2 2.012(5)	N2 Cu O2 165.8(2)	C12 C11 O2 119.3(6)
Cu N2 1.896(5)	N2 Cu O2 91.8(2)	C12 C11 C10 118.6(6)
O1 C1 1.303(9)	C1 O1 Cu 108.5(4)	C13 C12 C11 121.6(6)
O2 C11 1.346(8)	C11 O2 Cu 132.8(4)	C12 C13 N3 121.4(6)
N1 N2 1.400(7)	C11 O2 Cu 125.9(4)	C14 C13 N3 119.5(7)
N1 C1 1.304(9)	C1 N1 N2 108.8(5)	C14 C13 C12 119.1(6)
N2 C9 1.292(9)	N1 N2 Cu 115.9(4)	C15 C14 C13 118.2(7)
N3 C13 1.379(9)	C9 N2 Cu 128.9(5)	C14 C15 C10 124.4(7)
N3 C16 1.457(10)	C9 N2 N1 115.2(5)	C17 C16 N3 114.1(7)
N3 C18 1.456(10)	C16 N3 C13 121.5(6)	C19 C18 N3 113.6(7)
C1 C2 1.487(9)	C18 N3 C13 120.7(6)	
C2 C3 1.395(10)	C18 N3 C16 117.4(6)	
C2 C7 1.397(10)	N1 C1 O1 125.2(6)	
C3 C4 1.391(10)	C2 C1 O1 119.5(6)	
C4 C5 1.384(11)	C2 C1 N1 115.3(6)	
C5 C6 1.395(11)	C3 C2 C1 120.4(6)	
C5 C8 1.508(10)	C7 C2 C1 121.1(7)	
C6 C7 1.378(10)	C7 C2 C3 118.5(6)	
C9 C10 1.420(9)	C4 C3 C2 120.6(6)	
C10 C11 1.416(9)	C5 C4 C3 121.2(7)	
C10 C15 1.386(10)	C6 C5 C4 117.6(6)	
C11 C12 1.409(9)	C8 C5 C4 121.0(7)	
C12 C13 1.409(10)	C8 C5 C6 121.4(7)	
C13 C14 1.405(10)	C7 C6 C5 122.1(7)	

C14 C15 1.378(10)	C6 C7 C2 120.0(7)	
C16 C17 1.509(12)	C10 C9 N2 125.2(6)	
C18 C19 1.533(11)	C11 C10 C9 125.1(6)	

Table S4 Selected bond lengths (Å) and bond angles (°) for **L**

Bond lengths (Å)	**Bond angles (°)**	**Bond angles (°)**
C101 C106 1.389(2)	C106 C101 C102 118.22(16)	O22 C210 C209 121.56(15)
C101 C102 1.396(2)	C106 C101 C107 118.54(15)	C211 C210 C209 120.97(16)
C101 C107 1.491(2)	C102 C101 C107 123.23(15)	C210 O22 H12B 106.1(16)
C102 C103 1.383(2)	C103 C102 C101 120.38(16)	C210 C211 C212 121.40(16)
C103 C104 1.390(2)	C102 C103 C104 121.55(16)	N23 C212 C211 121.31(16)
C104 C105 1.388(2)	C105 C104 C103 117.89(16)	N23 C212 C213 121.02(16)
C104 C4A 1.506(2)	C105 C104 C4A 121.59(16)	C211 C212 C213 117.67(16)
C105 C106 1.387(2)	C103 C104 C4A 120.51(16)	C214 C213 C212 120.81(17)
C107 O11 1.239(2)	C106 C105 C104 120.98(17)	C213 C214 C209 121.96(16)
C107 N11 1.349(2)	C105 C106 C101 120.95(16)	C212 N23 C215 120.98(16)
N11 N12 1.3767(19)	O11 C107 N11 121.49(16)	C212 N23 C217 122.60(15)
N12 C108 1.286(2)	O11 C107 C101 122.57(15)	C215 N23 C217 116.24(15)
C108 C109 1.440(2)	N11 C107 C101 115.93(14)	C212 N23 C15' 117.7(4)
C109 C114 1.397(2)	C107 N11 N12 119.18(14)	C217 N23 C15' 109.4(4)
C109 C110 1.407(2)	C108 N12 N11 117.34(14)	N23 C215 C216 111.38(19)
C110 O12 1.363(2)	N12 C108 C109 120.38(15)	C16' C15' N23 104.0(9)
C110 C111 1.381(2)	C114 C109 C110 116.98(16)	N23 C217 C218 113.04(16)
O12 H12A 0.91(3)	C114 C109 C108 120.73(15)	
C111 C112 1.405(2)	C110 C109 C108 122.29(15)	
C112 N13 1.376(2)	O12 C110 C111 117.57(15)	
C112 C113 1.416(2)	O12 C110 C109 121.17(15)	
C113 C114 1.373(2)	C111 C110 C109 121.25(16)	
N13 C115 1.451(2)	C110 O12 H12A 106.0(16)	
N13 C117 1.460(2)	C110 C111 C112 121.28(15)	
C115 C116 1.522(3)	N13 C112 C111 121.68(15)	
C117 C118 1.516(3)	N13 C112 C113 120.87(16)	

C201 C202 1.389(2)	C111 C112 C113 117.44(16)	
C201 C206 1.393(2)	C114 C113 C112 120.40(16)	
C201 C207 1.492(2)	C113 C114 C109 122.57(16)	
C202 C203 1.389(2)	C112 N13 C115 121.33(14)	
C203 C204 1.392(3)	C112 N13 C117 121.00(15)	
C204 C205 1.393(3)	C115 N13 C117 117.67(14)	
C204 C4B 1.510(2)	N13 C115 C116 113.91(16)	
C205 C206 1.385(2)	N13 C117 C118 113.87(15)	
C207 O21 1.2283(19)	C202 C201 C206 119.42(16)	
C207 N21 1.352(2)	C202 C201 C207 123.07(16)	
N21 N22 1.3831(19)	C206 C201 C207 117.51(15)	
N22 C208 1.285(2)	C203 C202 C201 119.85(17)	
C208 C209 1.446(2)	C202 C203 C204 121.23(17)	
C209 C214 1.403(2)	C203 C204 C205 118.27(16)	
C209 C210 1.412(2)	C203 C204 C4B 121.54(17)	
C210 O22 1.356(2)	C205 C204 C4B 120.17(17)	
C210 C211 1.383(2)	C206 C205 C204 120.94(17)	
O22 H12B 0.93(3)	C205 C206 C201 120.22(16)	
C211 C212 1.399(2)	O21 C207 N21 122.91(15)	
C212 N23 1.371(2)	O21 C207 C201 122.23(15)	
C212 C213 1.411(2)	N21 C207 C201 114.84(14)	
C213 C214 1.373(2)	C207 N21 N22 118.30(13)	
N23 C215 1.455(3)	C208 N22 N21 116.94(14)	
N23 C217 1.461(2)	N22 C208 C209 120.56(15)	
N23 C15' 1.703(13)	C214 C209 C210 117.16(15)	
C215 C216 1.520(4)	C214 C209 C208 119.92(15)	
C15' C16' 1.481(17)	C210 C209 C208 122.92(15)	
C217 C218 1.517(3)	O22 C210 C211 117.47(15)	

Table S5 FTIR data (cm^{-1}) of free bilirubin and Cu(II)-bilirubin adduct

Vibration mode	Bilirubin	Cu(II)-bilirubin adduct
$\nu_{N\text{-}H}$	3406	3443
$\nu_{N\text{-}H}$ (lactum)	3267	3443
$\nu_{N\text{-}H}$	3008	2951
$\nu_{N\text{-}H}$	2912	2921
$\nu_{C\text{-}H}$	2856	2849
$\nu_{C=O}$ (COOH)	1695	1682
$\nu_{C=O}$ (lactum)	1645	1650
$\nu_{C=C}$	1611	1598
$\nu_{C=C}$	1568	1559
Ring torsion	1499	1508
Bridge carbon deformation, ring torsion	1445	1474
ν_{C-N}, CH_3 bending	1406	1388
ν_{C-H} bending (CH_3)	1364, 1345	1345
Bridge C–H bending, bridge $\nu_{C=C}$, ν_{C-N},	1300	1289
Ring	1250	1266
$\nu_{C\text{-}C}$	1219	1240
Ring breathing	1188	1223
Ring C-N	989	1023

Table S6 Effect of different solvents on oxidation of diphenyl sulphide catalyzed by **V1**[a]

Entry	Solvent	H_2O_2 (mmol)	Conversion (%)[b]	Selectivity of sulfoxide (%)[b]
1	Methanol	10	70	89
2	DMF	10	78	76
3	**Acetonitrile**	**10**	**97**	**98**
4	$CHCl_3$	10	10	51
5	Toluene	10	9	59
6	CH_3CH_2CN	10	48	86
7	iPrOH	10	30	61
8	Acetonitrile	5	93	80
9	Acetonitrile	15	95	65
10[c]	**Acetonitrile**	**10**	Trace	Trace

[a]Reaction conditions: diphenyl sulfide (5 mmol); 30% aqueous H_2O_2 (10 mmol); solvent (10 mL); 0.050g catalyst. [b] Conversion and selectivity were determined by GC. [c]Without catalyst.

Table S7 The effect of base and solvent on the **C1** catalyzed C-S cross coupling reactions[a]

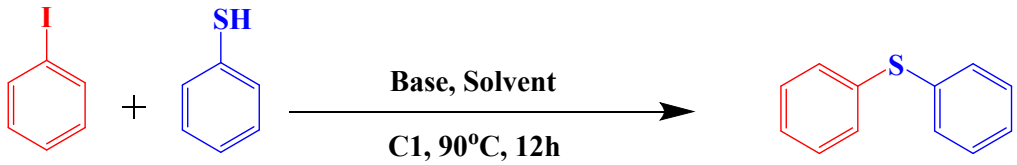

Entry	Base	Solvent	Yield (%)[b]
1	K_2CO_3	DMSO	73
2	K_2CO_3	DMF	86
3	**K_2CO_3**	**H_2O**	**98**
4	Cs_2CO_3	H_2O	82
5	KOH	H_2O	58
6	Et_3N	H_2O	34
7	Pyridine	H_2O	12
8	None	H_2O	None
9[c]	**K_2CO_3**	**H_2O**	Trace

[a]Reaction conditions: Iodobenzene (1 mmol), Thiophenol (1.1 mmol), water (3 mL), base (2 mmol), **C1** (15mg),Temperature (90^0C), Time (12h). [b] Yields were determined by GC and GCMS analysis. [c]Without catalyst

Table S8 Comparison with reported bilirubin probes

Sl. No.	Medium	Sensing method	Mechanism	Detection Limit	Binding Constant	Ref.
1	PBS Buffer	Turn off	FRET	150 nM	4.5×10^3 M^{-1}	1
2	PBS buffer	Turn off	FRET	0.59 pM	8.95×10^4 M^{-1}	2
3	HEPES buffer	Turn off	IFE	1.26 pM	4.18×10^6 M^{-1}	3
4	Aqueous	Turn off	Synergetic effect of IFE and PET	1.75 mM	6.4×10^4 M^{-1}	4
5	DMSO:WATER(1:9)	Turn off	IFE	0.3 μg/mL	-	5
6	50 mM HEPES, 5% DMSO	Turn on	Fe^{2+}-mediated deoxygenation of N-oxide of the probe	76 nM	-	6
7	Phosphate buffer	Turn off	FRET	2.8 pM (pH, 7.4); 3.3 pM (pH, 9.0)	-	7
8.	Aqueous	Turn off	IFE	257.4 fM	-	8
9.	Aqueous	Turn off	Reductive PET	1.8 μM	-	9
10.	PBS buffer	Turn off	Analyte-induced aggregation	8.90 ± 0.34 nM	-	10
11	Aqueous	Turn off	Static quenching	1.1×10^{-7} M	4.0×10^4 M^{-1}	11
12	Aqueous chloroform (chloroform: water, 1: 4)	Turn on	Ligand displacement approach	1.15 nM	7.78×10^5 M^{-1}	**Present work**

References

1. T. Senthilkumar and S. K. Asha, *Macromolecules*, 2015, **48**, 11, 3449–3461.

2. Y. Du, X. Li, X. Lv and Q. Jia, *ACS Appl. Mater. Interfaces*, 2017, **9**, 36, 30925–30932.

3. S. Nandi and S. Biswas, *Dalton Trans.*, 2019, **48**, 9266.

4 P. Xu, H. W. Yang, J. L. Shi, B. Ding, X. J. Zhao and E. C. Yang, *RSC Adv.*, 2019, **9**, 37584.

5. V. Srinivasan, M. A. Jhonsi, N. Dhenadhayalan, K.C. Lin, D. A. Ananth, T. Sivasudha, R. Narayanaswamy and A. Kathiravan, *Spectrochim. Acta Part A: Mol. Biomol. Spectroscop.*, 2019, **221**, 117150.

6. E. Ahmmed, A. Mondal, A. Sarkar, S. Chakraborty, S. Lohar, N. C. Saha, K. Dhara and P. Chattopadhyay, *ACS Appl. Bio Mater*., 2020, **3**, 7, 4074–4080.

7. S. Ellairaja, K. Shenbagavalli, S. Ponmariappan and V. S. Vasantha, *Biosens. Bioelectron*., 2017, **91**, 82-88.

8. R.S. Aparna, J. S. A. Devi, N. John, K. Abha, S.S. Syamchand and S. George, *Spectrochim. Acta Part A: Mol. Biomol. Spectroscop.* , 2018, **199**,123-129.

9. K. Abha , J. Nebu , J. S. A. Devi , R.S. Aparna , R. R. Anjanaa , A. O. Aswathya , S. George, *Sens. Actuat. B: Chemical* , 2019, **282**, 300-308.

10. W. Xiao, D. Zhi, Q. Pan, Y. Liang, F. Zhou and Z. Chen, *Anal. Methods*, 2020, **12**, 5691-5698.

11. S. Karmakar, T. K. Das, S. Kundu, S. Maiti, and A. Saha, *ACS Appl. Bio Mater*., 2020, **3**, 12, 8820–8829.